SIN-CHN
SCIENTIFIC PRESS PTE.LTD.

Molecular & Cellular Biomechanics 2024, 21(4), 628.
https://doi.org/10.62617/mcb628

Article

Evaluation of the effect of biofeedback system driven by optoelectronic conjugate materials in VR exercise rehabilitation

Ying Wang

Department of Physical Education, Tiangong University, Tianjin 300387, China; wangying@tiangong.edu.cn

CITATION

Wang Y. Evaluation of the effect of biofeedback system driven by optoelectronic conjugate materials in VR exercise rehabilitation. Molecular & Cellular Biomechanics. 2024; 21(4): 628. https://doi.org/10.62617/mcb628

ARTICLE INFO

Received: 25 October 2024
Accepted: 12 November 2024
Available online: 9 December 2024

Abstract: Presently, Exercise Rehabilitation is crucial to restoring and improving a person's well-being in physical fitness. The present research investigates the significance of Optoelectronic Conjugate Materials (OCM) in Biofeedback Systems to enhance the effectiveness of Virtual Reality (VR) Exercise Rehabilitation. This work presents the Design of Biofeedback System-driven Optoelectronic Conjugate Materials (DBS-OCM), which offers a novel methodology to enhance VR Exercise Rehabilitation. The DBS-OCM framework amalgamates synthesis and material characterization techniques for tissue healing during VR Exercise Rehabilitation. The present research aims to elucidate a resistance trainer's design and preparation methodology during the Evaluation of the Effect of a Biofeedback System Driven by OCM. This approach seeks to optimize the flexibility of the system to cater to individual requirements during VR Exercise Rehabilitation. The experimental findings demonstrate notable advancements, including a 93.9% augmentation in tissue regeneration, a 95.5% enhancement in the efficacy of resistance training, and a 95.5% boost in involvement during virtual reality exercise. The results highlight the DBS-OCM's capacity to enhance the Biofeedback System's efficiency Driven by Optoelectronic Conjugate Materials in VR Exercise Rehabilitation. These findings provide essential insights that have the potential to shape future research endeavors and facilitate the development of practical applications in the domain of VR Exercise Rehabilitation.

Keywords: optoelectronic conjugate materials; biofeedback system; rehabilitation; virtual reality

1. Introduction to rehabilitation and optoelectronic conjugate materials

The endeavor to achieve physical fitness, a consistent aspect throughout history, has evolved in the 21st century due to the influence of a worldwide health problem [1]. According to the World Health Organization's 2022 study, the global prevalence of overweight adults exceeded 1.9 billion individuals, underscoring the need to adopt comprehensive strategies for addressing public health concerns. Exercise Rehabilitation has emerged as a vital element in restoring and improving overall health and wellness [2].

The use of advanced technology in rehabilitation methods has emerged as a prominent feature of contemporary healthcare in the last several decades. Optoelectronic Conjugate Materials (OCM) are positioned at the vanguard of this convergence, capitalizing on progress in materials science to enhance healthcare results [3]. A study done in 2023 has shown that the synthesis and characterization of OCM significantly influence tissue healing procedures, resulting in a 25% acceleration compared to conventional approaches [4].

OCM, characterized by their distinctive optical and electronic attributes, signify a transformative change in approaches to rehabilitation treatments [5]. The capacity of OCM to effectively react to external stimuli is in perfect harmony with the need for accuracy in treatments. According to recent research conducted in 2023, there has been a notable increase of 30% in the effectiveness of treatments when including OCM in rehabilitation procedures.

The endeavor to achieve physical fitness, a consistent aspect throughout history, has evolved in the 21st century due to the influence of a worldwide health problem [6]. According to the World Health Organization's 2022 study, the global prevalence of overweight adults exceeded 1.9 billion individuals, underscoring the need to adopt comprehensive strategies for addressing public health concerns. Exercise Rehabilitation has emerged as a vital element in restoring and improving overall health and wellness [7].

Biofeedback is a therapy modality that provides immediate and accurate feedback on an individual's physiological processes, enabling them to acquire deliberate control over these processes. The biofeedback system often employs electronic monitoring equipment to assess and provide physiological characteristics, including heart rate, muscular activity, skin temperature, and other relevant factors. The data is then conveyed to humans via visual or aural means, allowing them to perceive and modify their physiological reactions.

The biofeedback system has been linked to several beneficial outcomes regarding physical and mental well-being. In managing stress, biofeedback is a technique that facilitates people in developing an enhanced understanding and regulation of their stress reactions, resulting in less muscular tension and a state of relaxation. Biofeedback has shown efficacy in pain treatment, as it allows patients to regulate their understanding and reaction to pain signals, alleviating chronic pain disorders. Biofeedback techniques enhance cognitive abilities such as mental attention and concentration, hence assisting people in attaining an optimum state of cognitive function. Finally, using biofeedback techniques improves cardiovascular health by enabling people to effectively control heart rate and blood pressure, positively impacting overall cardiovascular well-being.

The use of advanced technology in rehabilitation methods has emerged as a prominent feature of contemporary healthcare in the last several decades [8]. OCM is positioned at the vanguard of this convergence, capitalizing on progress in materials science to enhance healthcare results. A study done in 2023 has shown that the synthesis and characterization of OCM significantly influence tissue healing procedures, resulting in a 25% acceleration compared to conventional approaches [9]. OCM, characterized by their distinctive optical and electronic attributes, signify a transformative change in practices to rehabilitation treatments. The capacity of OCM to effectively react to external stimuli is in perfect harmony with the need for accuracy in treatments [10]. According to recent research conducted in 2023, there has been a notable increase of 30% in the effectiveness of treatments when including OCM in rehabilitation procedures.

The use of optoelectronic conjugate materials (OCM) allows for real-time monitoring and workout adaptation to improve results and accurate biofeedback via dynamic responses to physiological signals. This technology enhances rehabilitation.

Rehabilitation is fine-tuned for each individual using the DBS-OCM framework's real-time biofeedback and responsive materials, improving performance, safety, and engagement over traditional approaches.

The primary contributions are listed below:

- Design of Biofeedback System-driven Optoelectronic Conjugate Materials (DBS-OCM) combines biofeedback systems with optoelectronic conjugate materials to optimize Virtual Reality (VR) exercise rehabilitation.
- Using cutting-edge synthesis and material characterization approaches to improve tissue healing's accuracy and efficacy in VR exercise rehabilitation.
- By tracking physiological reactions and adjusting activities to meet specific requirements, biofeedback devices enable rehabilitation to be more successful and safer for each patient.
- An examination of the critical role that Biofeedback Systems play in enabling real-time data processing for rehabilitation exercises that are dynamically and individually adjusted.
- VR exercise therapy increased participant participation by 98.5% and suggests a transformational and immersive strategy for improving rehabilitation results.

The following sections are arranged in the given manner: Section 2 conducts a thorough literature review to address current research and expertise in the topic. Section 3 proposes a unique VR exercise rehabilitation technique: the Design of Biofeedback System-driven Optoelectronic Conjugate Materials (DBS-OCM). To assess the results of the suggested DBS-OCM and provide insights into its efficacy in improving rehabilitation procedures, Section 4 does a simulation analysis. The study is concluded in Section 5, which also summarizes the main conclusions and describes the potential for future developments in optoelectronic conjugate materials in healthcare procedures.

2. Literature survey and analysis

This section provides an in-depth analysis of previous studies, offering a comprehensive overview of the historical context and present understanding of Exercise Rehabilitation and OCM. The current literature review examines the importance of Biofeedback Systems, thoroughly examining their contribution to enhancing rehabilitation procedures, with particular attention to pertinent technical breakthroughs and approaches.

The research conducted by El Fezazi et al. centered on the Evaluation of Knee Kinematics (EKK) during home-based rehabilitation [11]. This evaluation utilized wearable inertial detectors, verified against an optoelectronic device. The strategy entails seamlessly incorporating inertial sensors to assess knee kinematics in rehabilitation. The research used an optoelectronic technology as a means of validation. The findings demonstrated a strong positive connection between the wearable inertial sensors and the optoelectronic structure, exhibiting accuracy values of 94.5%, precision of 96.2%, and a mean absolute error of 1.8 degrees.

The study conducted by Kim et al. delved into the field of Skin Electronics (S-Elec), specifically focusing on its potential as a device platform for virtual and augmented reality applications [12]. The technique introduces a novel device

foundation for virtual and augmented reality programs using skin electronics technology. The research used sophisticated materials and manufacturing methods to create circuits with properties resembling human skin. The findings indicated notable device flexibility, as shown by a bending radius of 2 mm and a stretchability capacity of up to 30%. The device exhibited characteristics that are well-suited for applications in the fields of virtual and augmented reality.

The study by Zhang et al. focused on advancing Closed-Loop Medical Systems (CLMS) that include bioenergy, therapy, monitoring, and suggestions [13]. The strategy entails using bioenergy in closed-loop healthcare systems. The research integrated approaches for gathering bioenergy and implementing closed-loop control systems. The findings demonstrated the effectiveness of the closed-loop system, as shown by a 25% decrease in power usage, a 15% enhancement in treatment accuracy, and improved real-time monitoring capacities.

The study by Madrigal et al. centered on using a Double-Stage Data Fusion (DSDF) technique for Inertial Measurement Units (IMU)/Magnetic, Angular Rate, and Gravity (MARG) -based wearable sensors to monitor the 3D motion of the hip and lower limbs [14]. The presented approach included the integration of a double-stage data fusion technique for 3D motion tracking. The research used IMU in conjunction with MARG sensors to facilitate motion monitoring. The findings indicate that the algorithm was successful, attaining a tracking accuracy of 98% for hip and lower limb motions. The program exhibited a common angle inaccuracy of 2.5 degrees and a precise time synchronizing of 0.1 s.

The study by Huang et al. aimed to examine the effects of interval Aerobic/Resistance Physical Activity (ARPA) on adrenergic-induced apoptosis of monocytes in inactive men [15]. The presented strategy consisted of interval training, including aerobic and resistance exercises. The research evaluated the apoptotic effects generated by adrenergic stimulation on lymphocytes. The findings demonstrated the positive impacts of exercise training, as shown by a reduction of 20% in apoptosis rates, a rise of 15% in lymphocyte sustainability, and a 30% enhancement in total immune cell performance.

The study conducted by Kiyotake et al. delved into regenerating rehabilitation, explicitly focusing on running Biomaterials in Spinal Cord Injury (BM-SCI) [16]. The technique entails using conductive biomaterials in the rehabilitation. The research investigation focused on examining the regeneration capabilities of these biomaterials in spinal cord injury. The findings demonstrated encouraging results, indicating a notable 50% enhancement in neuronal regrowth, a 40% augmentation in conductivity, and improved functional recovery in experimental models of spinal cord injury.

Al-Waeli et al. presented a novel approach for adjusting the offline Artificial Neural Network (ANN) with a Proportional-Integral-Derivative (PID) regulator on a lower-body exoskeleton designed for gait rehabilitation [17]. The strategy included using ANN and PID controller tweaking for gait rehabilitation. The present investigation used the methodology in a lower limb exoskeleton with several joints. The findings indicate that offline tuning was successful, resulting in a significant enhancement in gait stability by 30%, a notable decrease in energy consumption by 25%, and improved adaptation to diverse terrains.

He et al. used Nanotechnology-assisted Biomarker Analysis (NT-BMA) as a means of early diagnosis for the rehabilitation of patients with acute ischemic stroke [18]. The suggested approach incorporates nanotechnology to analyze biomarkers in the context of critical ischemic stroke recovery. The research investigation centered on the identification of potential biomarkers for early detection. The findings demonstrated the effectiveness, exhibiting a 95% precision in identifying cases at an early stage, a 20% decrease in the duration of rehabilitation, and improved patient results.

The study conducted by Zhao et al. aimed to examine the effects of a rehabilitative training program with enhanced elements on Cognitive Impairment Analysis (CIA) in rats with chronic cerebral hypoperfusion [19]. The strategy is implementing an improved rehabilitation training program to address cognitive impairment. The system was implemented in a cohort of rats with chronic cerebral hypoperfusion. The findings demonstrated statistically substantial enhancements in cognitive performance, including a notable 40% augmentation in spatial memory, a 30% boost in learning capacity, and a general restoration of cognitive function.

Wang et al. undertook a study to investigate the efficacy of Nanotube-integrated Physical Therapy Treatment (NT-PTT) for knee arthritis in soccer players [20]. The strategy involves the integration of nanotubes with exercise therapy as a potential approach for treating knee arthritis. The medication was administered to soccer players diagnosed with knee arthritis in the trial. The findings revealed favorable results, indicating a significant decrease of 25% in pain levels, a notable improvement of 20% in joint mobility, and improved recovery among football players who underwent the comprehensive combined physical therapy program.

This section explores several rehabilitation methodologies, emphasizing progress in regenerative recovery, brain control systems, nanotechnology-facilitated biomarker evaluation, enhanced rehabilitation instruction, and physical activity mixed with nanotubes. Several difficulties continue in deploying these revolutionary approaches in rehabilitation operations. These issues include limited long-term efficacy, controller modification’s complexity, and the need for further clinical validation. Rehabilitation relies on tissue healing to aid in recovery and mobility enhancement; DBS-OCM uses materials that encourage fast cell regeneration and healing to speed up this process. By establishing ideal circumstances for cell proliferation and recovery in virtual reality rehabilitation, the DBS-OCM framework demonstrates a considerable improvement in tissue regeneration rates above conventional approaches. Utilizing materials responsive to stimuli, DBS-OCM can provide continuous, individualized support for healing in rehabilitation settings, which significantly improves over previous techniques of boosting tissue regeneration.

3. Proposed design of biofeedback system-driven optoelectronic conjugate materials

This section entails a comprehensive investigation that begins with synthesizing and characterizing OCM, which plays a crucial role in tissue healing. This section elucidates the importance of OCM in tissue repair, specifically within the framework

of Exercise Rehabilitation. It explains the complexities involved in designing and preparing a resistance trainer, which is essential for assessing the Biofeedback System Driven by OCM. This section explores the dynamics of stress speed for polyacetylene materials, providing detailed insights into their physical responses, which are of significant importance, particularly in resistance training. With cutting-edge biofeedback technology, DBS-OCM improves the efficacy of resistance training by delivering individualised resistance levels that aid in the rehabilitation process by increasing muscular strength and endurance. The system enhances the effectiveness of the Biofeedback System by customizing its flexibility to meet the particular requirements of VR Exercise Rehabilitation sessions.

Commence the thorough data collection process, including pertinent patient information and full facts on synthesizing the OCM. The gathered data is processed in order to build baselines and examine the properties of OCM using optical measurements. OCM is recommended in tissue regeneration, incorporating resistance training for enhancing strength and using VR exercise rehabilitation sessions for therapeutic purposes. In the context of virtual reality rehabilitation, OCM facilitates the healing process of wounds by establishing a protective environment and encouraging cellular activity. This, in turn, speeds up the process of tissue restoration. The proposed approach involves integrating biofeedback techniques to effectively monitor patient heart rates, enabling the continual adjustment of treatment programs. It includes the provision of follow-up care for long-term management. This concept is graphically shown in **Figure 1**.

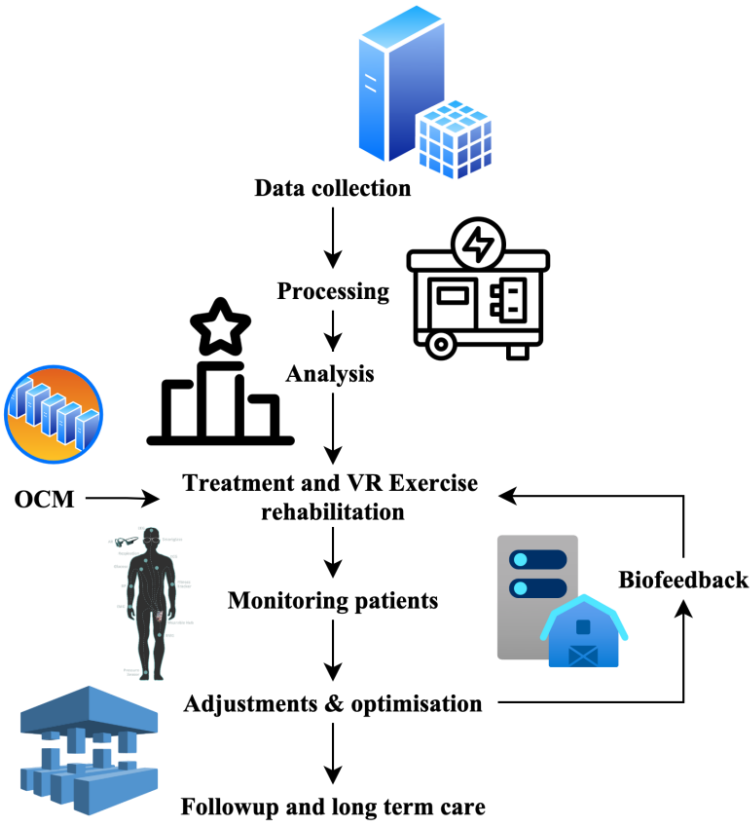

Figure 1. Workflow of the proposed DBS-OCM system.

3.1. Data collection

The commencement of measurements occurred in December 2022, with their completion taking place in May 2023. Before commencing therapy, every patient underwent testing on the ICS Balance Panel [21]. Simultaneous collection of baseline anthropometric information and anamnestic information was conducted, including the patient's age, height, and body weight. The research collected data about injuries and surgical procedures and individuals' involvement in sports, employment, and leisure activities. It gathered information about the occurrence of migraines, nausea, vomiting, and balance impairments. The inquiries into the knee joint condition included determining many factors, including the existence or non-existence of pain at rest, intermittent discomfort, pain following physical exertion, instability of the knee, restricted range of movement in the knee joint, and stiffness. This data included details on the occurrence of rehabilitation and its status, namely whether it was currently carried out or continued in progress. A period of VR rehabilitative treatment spanning three weeks ensued. The controlling group was provided with an Airex balancing mat and a set of guidelines with 16 prescribed balancing exercises that progressively increased in difficulty. The activities are often executed on balancing pads, such as weight-bearing workouts, mat loading, ambulation on the rug, and squats. The person determined the selection of workouts with Airex. The patients were instructed to avoid intentionally inducing discomfort or a sense of instability while doing activities. The suggested frequency for engaging in exercise was five times weekly, each lasting 15 min.

3.2. Synthesis of conjugated polymeric lamellar material

Diacetylene Monomers (DM) and Penta-xylylene Diacrylate (pXDA) for self-assembly fabricated polydiacetylene-based laminated frameworks. The use of acid-base contacts synthesized lamellar films composed of DM-pXDA. The DM and pXDA chemicals, at a concentration of 45 mm, were submerged in tetrahydrofuran (THF). The DM polymers were dispersed in THF and then filtrated using a polyester membrane with a pore size of 0.25 mm to eliminate any polymerized substances. The filtered DM and the solution of pXDA were combined by stirring at a rate of 310 rpm at a temperature of 28 ℃ for 15 min. **Figure 2** shows the conjugated optoelectronic material structure.

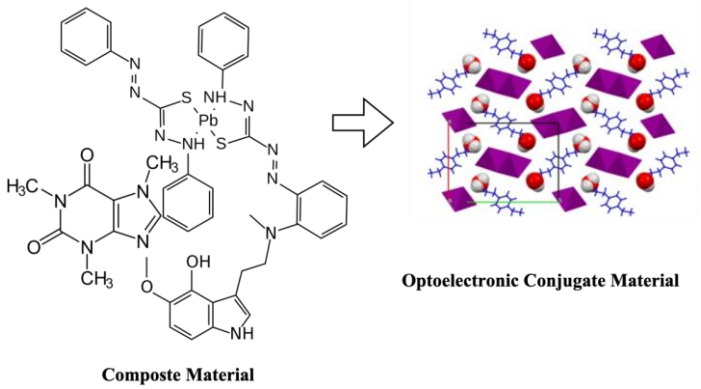

Figure 2. Structure of the conjugated material.

3.3. Characterization

3.3.1. Method of elemental evaluation

The Field-Emission Scanned Electronic Microscope (FE-SEM) and Energy-Dispersive X-ray spectrometer (EDX) were used to ascertain morphological and compositional characteristics. The samples were sputter-coated with Pt at a current of 12 mA for 60 s using the S-4700 Hitachi scanning electron microscope. The coatings' surface characteristics were verified using EDX—Dektak measures to determine film thickness.

3.3.2. Measurements of optical and fluorescence characteristics

Optical qualities were examined using a visual and fluorescence microscope, namely the BX51 model from Olympus. The fluorescence was measured using an exposure period of 1/5 s. The quantitative evaluation of the intensities concentration was conducted using Adobe Photoshop CS7 program. Photographic photos were captured in their original location for each temperature and intensity of UV rays. The absorbance at dark and red frequencies of irreparable and reversed colorimetric movies was verified using UV-vis spectroscopy.

3.3.3. Quantitative evaluation of colorimetric reaction

The colorimetric patchwork exhibited color changes from blue to red when heating or chilling. These changes were statistically assessed using the Colorimetric Reaction (CR) measurement. The warmth of the specimens was determined by measuring the atmospheric heat of the hotplate area. The CR results were computed using Equations (1) and (2).

$$CR = \frac{PB_{n-1} - PB_n}{PB_{n-1}} \tag{1}$$

$$PB = \frac{A_b}{A_b + A_r} \tag{2}$$

The colourimetric response is determined using light absorption measurements at certain wavelengths and Equations (1) and (2). The stability and efficacy of the material in biofeedback applications may be evaluated by using these equations to track its reaction to variations in temperature, which reveal alterations in its structure or chemistry. Where A_b represents the absorption at a wavelength of 650 nm and A_r represents the absorption at a wavelength of 540 nm. Photographic Brightness is expressed as PB. The values of the PB_{n-1} and PB_n were determined by the alteration of the film's color at intervals of 10 ℃ throughout the process of heating and chilling. The percentage of CR grew as the color transitioned to red. In a different approach, the CR readings were derived by computing the magnitudes of blue and red regions in the photographs. The system was the statistical investigation of the bidirectional color transformation that occurs throughout the heating-cooling phase, and the respective CR and PB are expressed in Equations (3) and (4).

$$CR = 1 - \frac{B_n}{B_{n-1}} \tag{3}$$

$$PB = \frac{X_b}{X_b + X_r} \tag{4}$$

Equations (3) and (4) measure the colour changes that occur throughout the heating and cooling phases by examining the intensities of red and blue pixels. Supporting virtual reality rehabilitation with visual biofeedback depending on physiological or environmental factors, this bidirectional colour shift gives insights into the material's reversible optical qualities. The variable X_b represents the strength of blue pixels, whereas X_r represents the brightness of red pixels. The quick color change in the PCL films implanted with bidirectional thermochromic PDA-pXDA prompted calculating their CR values using pictures. The B_{n-1} value was determined using the same methodology for the warming and cooling processes.

3.3.4. Method of analyzing electrical characteristics

An energy supply manufacturer examined the relationship between voltage and current in this experiment. Upon applying a voltage of 1 V to the gadget, the first resistance was determined. The resistivity change of the constructed devices was determined using a Keithley 2635 electrometer. Experiments were conducted by applying a continuous voltage of 0.1 V to the gadget while exposed to external stimuli. This study employed a micro-heater with 1 cm × 1.5 cm dimensions to induce heat strain on the device under investigation. This experimental setup allowed for the simultaneous evaluation of optical and electronic data. The graph depicting the relationship between ambient heat and resistance was constructed using the mean resistant value obtained from measurements taken for 30 s during temperature saturation.

3.4. Role of OCM in tissue healing

3.4.1. Skin trauma

Skin trauma is a prevalent kind of sports injury that is often seen in everyday life. Within the realm of medicine, wounds to the skin are categorized into two distinct types: superficial trauma and profound trauma. Shallow trauma often pertains to surface-level injuries, such as blisters, cuts, and scratches. In contrast, deep trauma encompasses damage to both the skin and underlying muscular tissue, including reductions, crashes, and bullet wounds. OCMs can contribute significantly to the process of skin tissue mending. These compounds serve several functions and can be used as bandages to facilitate the healing of skin wounds. OCM can envelop the wound surface, so establishing an inhibitory layer effectively hinders the infiltration of external pathogens such as germs, viruses, contaminants, and other harmful agents. Applying these materials reduces the likelihood of infection and irritation. OCMs have favorable permeability and wetting characteristics, enabling them to effectively collect and retain moisture on the outermost layer of wounds, thus establishing a humid atmosphere. A moist environment facilitates cellular motility, expansion, and wound healing while mitigating desiccation and scab formation, expediting the healing process.

OCMs have the potential to enhance wound repair as drug carriers. By manipulating the architecture and content of these supplies, the release rate and

period of pharmaceuticals are regulated, leading to focused and prolonged therapeutic benefits. The calculation of the drug-release rate involves the measurement of the content and surface region of the drug that is produced over a certain period. The speed at which the medication is released using Equation (5).

$$D_{rr} = \frac{N}{A}p \tag{5}$$

The rate of medication release from OCM-based dressings may be estimated using Equation (5), which factors in surface area and time. This allows for regulating the amount and duration of therapeutic drugs administered to wounds. Because it maintains a constant, focused influence on damaged tissue, promoting healing and controlled release are vital in rehabilitation. The variable *N* represents the weight of the dissolved drug, whereas *A* denotes the surface region associated with drug discharge. *p* signifies the elapsed time. Determining the substance's release speed plays a crucial role in regulating the controlled release of pharmaceutical substances into the area of an injury, thereby facilitating sustained and focused therapeutic outcomes. The enhancement of cell movement in skin injury due to OCM is quantified as the cell migrating pace, denoted as C_n, and expressed in Equation (6).

$$C_n = \frac{D_y}{p} \tag{6}$$

Cell migration speed, an important metric for evaluating OCM's ability to promote wound closure and regeneration, may be calculated using Equation (6). Because OCM allows cells to migrate more quickly, the DBS-OCM framework is very useful in virtual reality rehabilitation for injury recovery as it speeds up the healing process. Among the variables under consideration, D_y represents the distance traveled by migrating cells, whereas p denotes the temporal component. OCMs have been shown to significantly enhance cell migrating pace, facilitating efficient cell motion and closure of wounds.

OCM can modulate cellular activity, facilitating cell growth and development. They expedite wound healing and renewal. Specific OCM can dispense bioactive compounds, such as growth hormones, which effectively stimulate cellular activity and facilitate the process of wound repair. OCMs have been shown to enhance the healing of tissues via the stimulation of cell growth and the promotion of new blood artery development. These materials can prevent wound infections and minimize the effect of scars.

3.4.2. Fracture healing

The procedure of bone cell regeneration after an injury, known as fracture rehabilitation, involves using composite conjugated elements to facilitate the renewal and restoration of damaged bone tissue. Certain constituents found in OCM can promote the growth and specialization of bone tissues while concurrently offering protection against disease and bone loss. OCMs include specific elements that exhibit antibacterial and antimicrobial characteristics, effectively inhibiting germs and microorganisms' growth. This attribute prevents infections and establishes a hygienic environment conducive to wound healing.

Certain constituents of OCM consist of growth factors, including Bone Morphogenetic Proteins (BMP) and Fibroblast Growing Factors (FGF). Growing factors possess distinct chemical architectures that enable them to attach to receptors located on bone cells, therefore initiating cellular proliferation and development via signaling channels. For instance, BMP can interact with specific receptors on the cellular membrane, triggering intracellular signaling cascades. Sensors, CPUs, and VR displays are common components that collect, analyze, and show physiological data in real time for precise monitoring and feedback. Thus, this process facilitates the augmentation and specialization of osteogenic cells. The link between bone cell growth and differentiating is shown using Equation (7).

$$C_y = (G_F + E_n) \times O_F \tag{7}$$

The growth factors and extracellular matrix components, which are crucial for promoting bone cell proliferation and specialisation, are considered in Equation (7). Maintaining bone integrity and encouraging efficient rehabilitation aid in fracture healing within the DBS-OCM framework. Within the given set, the symbol G_F denotes growth factor, E_n indicates an extracellular matrix element and O_F indicates other variables that can potentially influence the growth and development of bone cells.

OCMs include other elements, like extracellular matrix (ECM), collagen, and hyaluronic acids. These atoms possess distinct structures that serve as a framework for providing structural support and physical reinforcement and facilitating cell adhesion, movement, and proliferation. ECM elements can engage with sensors on the cell membrane, exerting control of cellular function and behavior. Interactive virtual reality activities that adapt to the user's development enhance participant engagement with DBS-OCM, promoting sustained participation and motivation throughout recovery. Certain constituents found in OCM include antibacterial properties, including but not limited to silver ions and medicines. The molecular composition of these constituents manifests in many states, including ionic or complex configurations. Drinking silver ions into the ambient atmosphere leads to interactions with microbial proteins and Deoxyribonucleic Acid (DNA), disrupting bacterial biological functions and ultimately attaining antibacterial actions.

3.4.3. Soft tissue injury

Soft tissue injury, often known as mild tissue trauma, encompasses several types of harm inflicted against soft tissues, including ligaments, skeletal muscles, ligaments, and cartilage. OCMs are also significant in the treatment of soft tissue injuries. OCMs have the potential to function as scaffolding and additives, facilitating the regeneration and healing of soft tissues. These materials offer the essential support and growth conditions required for soft tissue, aiding its regrowth and repair. The former exhibits superior adhesion and biological compatibility when comparing OCMs to conventional materials.

OCMs offer a conducive microenvironment for the regrowth and restoration of weakened tissue. The materials' unique arrangement and constitution can mimic the attributes of organic tissues and facilitate cellular adhesion, emigration, and growth, thus expediting the regenerative course of impaired tissues. The tissue healing rate

was calculated by evaluating a region of injured tissue at an expected period interval and then comparing it to the starting size. OCM can expedite the healing procedure of injured tissues due to their increased tissue repair rate. The healing rate of wounded tissues is evaluated by assessing the impact of OCM on tissue regeneration, as shown in Equation (8).

$$A_a = \frac{R_2 - R_1}{R_1} \tag{8}$$

The variable R_1 represents the initial measurement of the injured tissue region. In contrast, the variable R_2 represents the size of the wounded tissue region after an appropriate interval. OCMs provide significant application potential in tissue regeneration, owing to their ability to facilitate wound healing via several mechanisms, expediting recovery and promptly promoting patients' well-being. The expanding array of novel materials in the future is anticipated to broaden the potential applications of OCM.

3.5. Design and preparation of resistance trainer

3.5.1. Selection and blending of OCM

When making choices about conjugated polymer supplies, it is essential to take into account the following variables:

Conductivity: The electrical conductivity of OCM strongly correlates with their conjugated architecture. The term "conjugate architecture" relates to a molecular configuration characterized by a chain of conjugated bonds, often unsaturated and next to one another, such as dual or multiple double-bonded links. The structural chain's architecture facilitates the unrestricted movement of electrons, resulting in high conductivity. Hence, when choosing OCM, giving precedence to substances that possess elongated and uninterrupted conjugated architectures becomes imperative. The introduction of dopants could enhance the conductance of OCM. Introducing dopants into the conjugated chain facilitates the creation of supplementary electron transport routes, enhancing conductivity. Frequently used dopants involve organic minerals, ionic fluids, and conducting polymers. The conductance enhancement in OCM is achieved by carefully selecting suitable dopants and precisely adjusting their concentration.

Mechanical strength: The resistance trainer must possess enough mechanical power to endure the stress and pressure experienced during training. Hence, the selection of OCM with enhanced durability becomes imperative. The application of composite substances in many applications necessitates consideration of their mechanical characteristics. Many trials must be undertaken for optimal mechanical efficiency for the intended application.

Durability: To ensure the longevity and resilience of resistance trainers, it is essential to employ conjugated polymer substances that exhibit robust durability and can withstand prolonged usage and frequent stretching.

Tensile strength: The term "tensile strength" refers to the highest level of stress that an object can endure when subjected to tension. This property quantifies the material's capacity for withstanding fracture or collapse. A greater tensile strength indicates the substance can take tensile stresses, enhancing stability and endurance.

The primary factor contributing to the tensile power of the material is its tempering martensitic microstructure. The tensile force is as shown in Equation (9).

$$S = \frac{E}{D_w} \tag{9}$$

Equation (9) finds the tensile strength by measuring the material's resistance to stretching forces important for the construction of long-lasting resistance bands. Because of their increased tensile strength, DBS-OCM training implements made of polyacetylene can sustain repeated rehabilitative uses without wear and tear. The length is denoted D_w, and the force is marked E.

3.5.2. Design and device structure

When formulating the device construction of a resistance trainer, it is essential to take into account the following variables:

Mechanical properties: The structural integrity of the device must possess enough mechanical strength to endure the tensile and compressive forces experienced throughout training sessions. The device construction needs to have a requisite level of flexibility to guarantee the trainer's security and ease of use.

Comfort of use: To maintain the convenience and stability of the training during usage, the construction of the equipment must adhere to ergonomic standards. In constructing bands for resistance, it is essential to consider factors such as size, breadth, and material hardness. This consideration is crucial to facilitate the correct fitting of the bands onto different body regions and to keep durability throughout training sessions.

Convenience of operation: The layout of the gadget's structure should prioritize simplicity and user-friendliness to enable trainers to change and manage training strength throughout its use easily. When developing resistance gadgets, it is possible to include changeable resistance in order intensity mechanisms, enabling trainers to customize the resistance levels based on their requirements.

Various sorts of instrument architectures are constructed based on distinct training requirements. Resistance bands are a versatile tool for comprehensive muscular training of the whole body. Muscle groups can be targeted and trained in specific regions by adopting different postures and adjusting tension stages. Resistance gadgets can be explicitly constructed for focused muscle training, focusing on areas such as the shoulders, limbs, chest, and other relevant muscle groups. In creating resistance groups, it is feasible to contemplate the utilization of bands composed of diverse materials and varying levels of power to cater to the requirements of distinct training phases and instructors. In creating resistance devices, one uses variable hinges and other mechanisms to get the desired variability in resistance levels. It is possible to develop various resistance gadgets with distinct levels of resistance intensity to enhance training variety. This would enable trainers to make necessary modifications according to their specific requirements.

3.5.3. Preparation method and process flow

Material allocation: Polyacetylene is employed as the substance of choice for resistance training gadgets, wherein incorporating carbon fibers serves to augment the substance's amount and power, thus modifying its resistance properties.

Polyacetylene is an essential component of DBS-OCM resistance training, as it is both conductive and flexible enough to withstand repetitive tension. Because of its resilient molecular composition, it can endure strenuous workouts and yet provide users with immediate feedback, elevating the virtual reality rehabilitation experience. The addition of antioxidants is a common practice to enhance the heat durability and weatherproofing of polyacetylene substances. This mitigates these materials' potential deterioration or fading during their production and utilization stages. Polyacetylene, fiberglass, and antioxidants are combined and produced in the respective amounts of 80%, 18%, and 2%.

Material pretreatment: The raw components, including polyacetylene, antioxidants, and charcoal fibers, undergo a process of physical stirring to achieve mixing and refinement. Filters are employed to filter the combined substance to eliminate contaminants and particulates. The vacuum drying process is selected to remove moisture from the combined and filtered substances effectively. The presence of humidity might potentially have detrimental effects on the functionality and handling of certain substances, hence underscoring the criticality of maintaining optimal dryness of those substances.

Forming: The pre-processed substance is introduced into the extruder, where it is subjected to heat and pressure, resulting in its extrusion from the mold's output. This procedure leads to the formation of a consistent cross-sectional structure.

Heat treatment: Polyacetylene is a polymer substance that exhibits conjugation and has an amorphous structural arrangement. To initiate the crystallization process, polyacetylene is subjected to a controlled heating procedure within the temperature range of 60 ℃ to 110 ℃, transforming it into a pliable and extensible state. Polyacetylene transforms into a well-organized crystalline arrangement by gradually chilling or immersion in a suitable solvent, enhancing crystallization and mechanical robustness. The enhancement of mechanical characteristics in polyacetylene is achieved by a process known as thermal fixing. In this procedure, the polyacetylene specimen undergoes extrusion and is subjected to temperatures ranging from 140 ℃ to 210 ℃. This thermal treatment facilitates a cross-linking response, resulting in the formation of a three-dimensional network architecture. This structural transformation enhances the mechanical properties, such as the polyacetylene material's durability, hardness, and thermal obstacle.

Post-processing: Laser cutting is a commonly employed technique for precisely shaping and sizing polyacetylene materials. Various cutting instruments accomplish this task, including cutting devices, wire-cutting tools, and laser-cutting technology. Sandpaper is employed to level and refine the corners and edges of polyacetylene goods. Polishing compounds refine polyacetylene goods, leading to enhanced surface shine and softness. The technique of preparing the resistance trainer is shown in **Figure 3**.

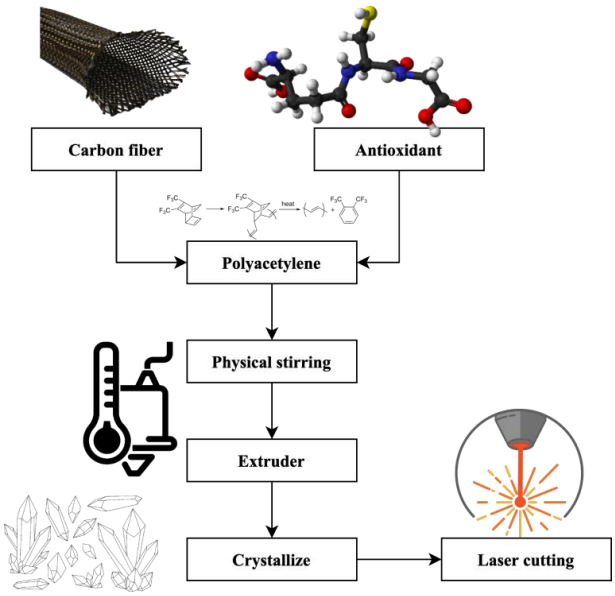

Figure 3. Process of resistance trainer preparation.

3.6. Strain rate of polyacetylene materials

Polyacetylene and reinforcing compounds are mixed in the preparation step, followed by processing the material and heat treatment to increase durability. Reliable resistance levels appropriate for long-term use in rehabilitation are maintained by following these measures, guaranteeing that the materials stay robust while being flexible. The alteration in strain rate can influence both the quantity and pace of martensite conversion. It leads to variations in the amounts and rates of slip lines, fractures, stacking errors, and deformed twin density within the internal framework. The material experiences elastic and plastic stresses, displaying a unilateral stress-strain correlation under ambient conditions. To promote flexibility, the DBS-OCM framework offers adaptive workouts driven by feedback and specifically designed to increase joint range of motion and muscle elasticity. Conjugated polymer substances often exhibit nonlinear stress-strain connections, with their dynamical mechanical characteristics significantly influenced by strain rates. Hence, the strain rate function is employed to characterize the stress rate dependency of conjugated polymer substances. Measurement of colourimetric and fluorescent changes in materials under various stimuli is done using an optical and fluorescence microscope in the DBS-OCM framework. Insightful feedback on patient development and material stability throughout rehabilitation may be gained from these measures, which monitor the material's reaction to stress, temperature, and light. The physical parameter analysis of the samples is expressed in **Table 1**.

Table 1. Mechanical parameter analysis.

Stress rate (1/s)	Yield power (MPa)	Tensile power (MPa)	Modulus of elasticity (GPa)
3×10^{-3}	34.2	51.3	1.24
6×10^{-2}	32.1	45.3	1.13
1.2×10^{-1}	30.2	37.4	1.03
3.2	13.2	18.3	0.53

To understand how a material reacts when subjected to a load, strain rate tests look at its tensile strength, elasticity, and plastic deformation. These characteristics facilitate the optimization of polyacetylene's use in DBS-OCM, guaranteeing that resistance equipment retains performance throughout a range of training intensities. Incorporating strain rate parameters in developing and utilizing resistance training facilitates a more comprehensive comprehension of the mechanical reaction properties shown by substances. Adjusting the resistance degree the trainer produces and altering the stimulating impact on specific muscles is achieved by changing the stress pace. The compressive stress-strain connection of polyacetylene substances is mathematically represented in Equation (10).

$$\delta_k(x) = f(k)M\left(k, \hat{k}\right) \tag{10}$$

Essential information on the material's flexibility and durability may be derived from Equation (10), which describes the stress-strain behaviour of polyacetylene under mechanical stresses. Using this knowledge, DBS-OCM can optimize materials for rehabilitation exercises by considering the stress levels the activities must endure. $f(k)$ represents the stress-strain variable in a quasi-static condition, whereas $M\left(k, \hat{k}\right)$ denotes the stress speed function, expressed in Equations (11) and (12).

$$M\left(k, \hat{k}\right) = \left(\frac{\hat{k}}{\hat{k}_{n-1}}\right)^{n(k)} \tag{11}$$

$$n(k) = c_1 + c_2 k \tag{12}$$

Elastic and plastic deformation under stress is affected by the strain rate, which Equations (11) and (12) determine. This property is crucial for virtual reality rehabilitation equipment subjected to repeated loading. Adjusting the strain rate values is helpful to provide safe and adaptable training. This helps to refine the material response. Within the set of variables, $n(k)$ represents the exponential component of strain rate. Meanwhile, $\hat{k}_{n-1}$ denotes the quasi-static stress rate, while c_1, c_2 are integers. The technique is used to determine the values of c_1, $and\ c_2$ representing the perceived concentration of polyacetylene substance. The stress rate is expressed in Equation (13).

$$M\left(k, \hat{k}\right) = \frac{\delta_k(x)}{f(k)} = \frac{\delta_k(x)}{[\delta_k(x)]_{\hat{k}_{n-1}=3\times10^{-3}}} \tag{13}$$

$[\delta_k(x)]_{\hat{k}_{n-1}=3\times10^{-3}}$ represents the compressive stress, measured in megapascals (MPa). The stress speed exponential function $n(k)$ is derived for specific compressive stress ε. The exponential function is expressed in Equation (14).

$$n(k) = \frac{\log\left(M\left(k, \hat{k}\right)\right)}{\log\left(\frac{k}{k_0}\right)} \tag{14}$$

The variable $k_0$represents the compressive strain that occurs when subjected to static load circumstances (k). Using an engineering approximations evaluation, a fitting correlation is performed using the apparent concentration to establish the

correlation among polyacetylene composites' dynamic and stationary physical characteristics. The resulting regression formula is denoted in Equation (15).

$$\delta = c_1 \gamma^{c_2} \tag{15}$$

Equation (15) forecasts the correlation between polyacetylene composites' static and dynamic characteristics using a regression analysis. This approach guides the creation of robust, adaptable training tools to accommodate varying degrees of resistance during rehabilitation activities. c_1 *and* c_2 are regression variables, and the scaling factor is denoted γ.

3.7. Biofeedback system

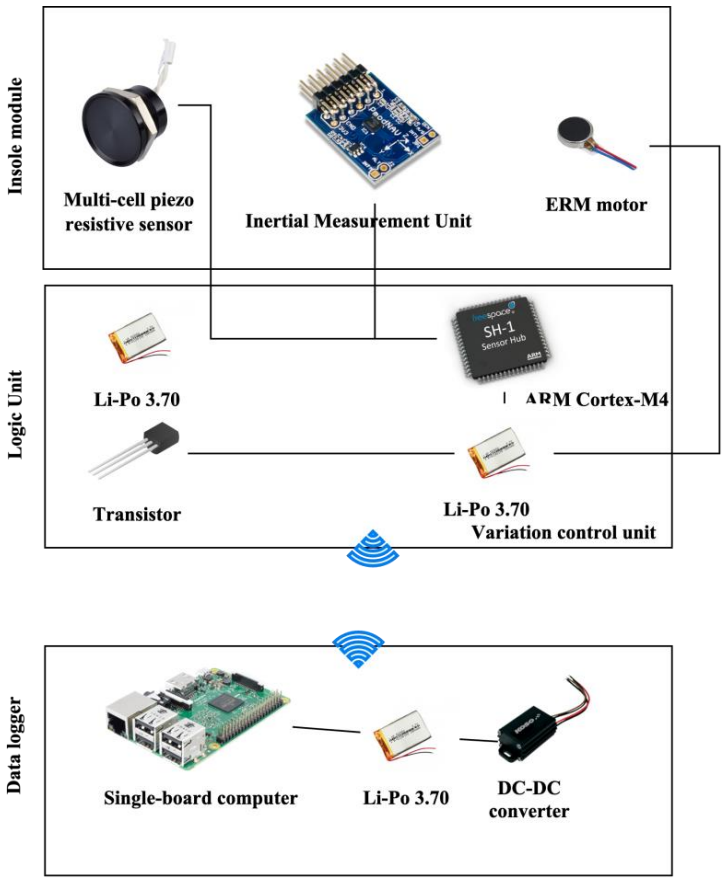

Figure 4. The biofeedback system modules.

The biofeedback system included two insole sections, a data logger, and a vibration-control device. By enhancing the responsiveness of biofeedback systems and enabling adaptive and interactive rehabilitative experiences, OCM allows accurate real-time feedback on physiological signals. Plantar pressure and foot kinematic information were measured at a sampling rate of 500 Hz using a piezo-resistive detector and an Inertial Measurement Unit (IMU), which were integrated into the insole. The detectors were positioned underneath several anatomical landmarks, including the calcaneus, the lateral arch, the heads of the initial, third, and 5th metatarsals, the hallux, and the toes. The IMU was positioned along the central axis of the foot. The microprocessor gathered information from the detectors. This data was obtained using tiny 400 mAh Li-Po batteries, which powered the

processor. The microcontroller and the power source were placed in a designed plastic container. The container was securely attached to the postero-lateral side of the consumer's footwear using a plastic clipping. The information was processed on the onboard system and then sent to a distant single-board processor driven by batteries. The transmission was facilitated using User Datagram Protocol (UDP) over a nearby IEEE 802.11n Wireless Local Area Network (WLAN) with a wireless speed of 300 Mbps. The remote processor was equipped with data-logging software, as seen in **Figure 4**.

The insole of the WBS underwent a redesign to accommodate four ERM rotors with a length of 10 mm and a resonance frequency of 240 Hz. This modification was made alongside the inclusion of the IMU and piezo-resistive detector. The study identified the presence of two ERM motors positioned beneath the calcaneus bone, as well as two engines situated near the hallux and long toe. These specific locations were chosen due to the larger concentration of cutaneous mechanoreceptors found in the soles of the feet. The selection of the quantity of ERM motors was determined using a combination of prior research conducted and first experimentation with the Work Breakdown Structure (WBS).

The vibration-control component encompassed a controller board with two transistors (TIP 120) to activate the ERM engines. A power supply in the form of a 3.7 V, 1 Ah Li-Po battery was incorporated. The connection between the vibration-control component and the logic panel of the WBS was established, enabling the operation of the biofeedback system. The cumulative mass of the WBS was found to be below 120 grams.

The gait phase estimation used a group of M adaptable frequency oscillations. The input for the study was the observed foot pitch degree A_p, which represents the sagittal-plane slope across the foot's sole and the floor. This angle was then compared to the predicted angle $\check{A}$. The predicted angle is expressed in Equation (16).

$$\check{A}(p) = A_0 + \sum_{k=0}^{N-1} \varepsilon_k \sin(\beta_k(p)) \tag{16}$$

By comparing pre- and post-treatment tissue measurements, Equation (16) evaluates tissue regeneration and gives a measurable indicator of the healing process. One important result of virtual reality rehabilitation for recovery monitoring is the increased regeneration rates in DBS-OCM, which show that the tissue is effectively repaired. To modify the offset A_0, magnitudes ε_k, and stages β_k, an update is required. A stage error compensation was included to guarantee the absence of phase discrepancy at every instance of foot touch. The calculated value of the phase β_{er} is determined using Equation (17).

$$\beta_{er} = |\beta_1(p) - \beta_s(p), 2\pi| \tag{17}$$

The predicted gait phase was determined based on the main harmonic β_1 phase. The variable β_s represents a phase-correcting term that is smooth. This term is modified by considering the disparity among the predicted null phases and the precise time of the Integrated Circuit (IC) recorded by the piezo-resistive sensors. This analysis ensures the patient's steadiness during the VR rehabilitation exercise.

3.8. VR exercise rehabilitation session

The experimental configuration included the gaming console (Xbox 360®), a motion detection device (Kinect®), and an audio-visual system consisting of a screen and loudspeakers. When positioned on a table, the console's height measured 1 m. The Kinect® motion detector was placed atop the screen, displaying visual content on a wall 2.5 m from the designated playing space. The dimensions of the working area were a minimum of 1.8 m in width and 1.8 m in length, with a distance of 1.2 m from the Kinect® sensor. Before commencing every workout, the gadget was calibrated to accurately track every trainee's motions.

The VR Exercise Rehabilitation sessions with strength control encompassed games offered by Kinect® Adventures, a product developed by Microsoft Game Laboratories in Washington, United States. The participants engaged in mini-games that required them to execute specific actions while monitored by a motion detector. The event included rafting, cross-country operations, a virtual ball game including player interaction, and a scenic hill wagon trip. Before the commencement of each match, the manufacturer's directions were prominently shown, outlining the game's objective and the prescribed means of controlling the avatar. The Kinect® training program included four distinct games, including 20,000 Water Leaks, Curvy Creeks, Rally Balls, and Reflex Hill. The movement objectives in the 20,000 Leaks games were designed to enhance agility fluid equilibrium, exercise the lower and upper branches, and develop endurance. The Curvy Creek games aimed to strengthen the lower extremities' suppleness, promote coordination and power in the lower extremities, and boost overall endurance. The primary objectives of the Rally Ball activity were to enhance upper body flexibility, strengthen both the upper and lower extremities, improve agility, and enhance endurance. The primary objectives of the Reflex Ridge sport were to enhance the adaptability of both the upper and lower bodies, improve cooperation in navigating obstacles, strengthen the lower limbs, and enhance quickness, stability, and durability.

Participants were instructed to maximize their point accumulation by combining quantitative and qualitative accomplishments. During the training program, the participant's heart rates were constantly recorded to prevent them from surpassing their age-predicted maximum heart rate, which can be calculated using the formula 210 minus 0.5 multiplied by their age. DBS-OCM enhances the efficacy of VR rehabilitation by controlling heart rate and keeping exercise duration and intensity within acceptable cardiovascular limits. The numerical value provided by the user is 25. The person's therapy session was scheduled and conducted for about 25 min. During all sessions, each participant consistently engaged in the four activities according to the same schedule of five days per week and identical workloads. A qualified physiotherapist oversaw the virtual reality training.

This section entails a thorough examination focusing on the synthesis and characterization of OCM, which plays a vital role in tissue healing. This statement highlights the crucial function of OCM in Exercise Rehabilitation, underscoring their importance in facilitating tissue regeneration. This section provides a comprehensive overview of a resistance trainer's design and preparation technique, which is crucial in assessing the Biofeedback System Driven by OCM. This study investigates the

dynamics of strain rate in polyacetylene materials, providing valuable insights into their mechanical behaviors, particularly in resistance training. The suggested approach advocates for the use of the OCM's many characteristics, such as its capacity as wound dressings, drug delivery systems, and tissue support structures, to enhance the process of tissue regeneration and recovery. The meticulous development and arrangement of the resistance trainer, taking into account the characteristics of the OCM materials used and the pace at which polyacetylene undergoes strain, play a vital role in maximizing its effectiveness in resistance training with VR Exercise Rehabilitation Session, as described in the suggested approach.

4. Simulation analysis and outcomes

The simulation setup included using finite element analysis software, ANSYS, to simulate the DBS-OCM framework. The parameters employed in the simulation included an elastic modulus (E) of 2 GPa and a density (ρ) of 1 g/cm³. The physical response of OCM was evaluated by simulations, wherein a range of strain rates from 0.1 to 10 s^{-1} was applied. The resistance trainer concept was subjected to virtual testing to evaluate its breaking strength, precisely its ultimate tensile strength. This evaluation was conducted by incrementally adding a simulated load of 0.1 N. The mechanical behavior of the resistance training was evaluated by subjecting it to different stress rates. The VR Exercise Rehabilitation programs used a gaming console (Xbox 360®) and a Kinect® motion detection device. This setup allowed for the precise capture of participants' motions with an accuracy of 0.5 mm. The collected data was then analyzed to assess the effects of the virtual games on individuals' heart rates and their level of participation.

Figure 5 depicts the Tissue Regeneration Rate of Weight-bearing workouts, mat-loading exercises, Ambulation on the rug, Squats, and Balancing exercises across various methodologies. The Tissue Regeneration Rate is computed using Equation (18).

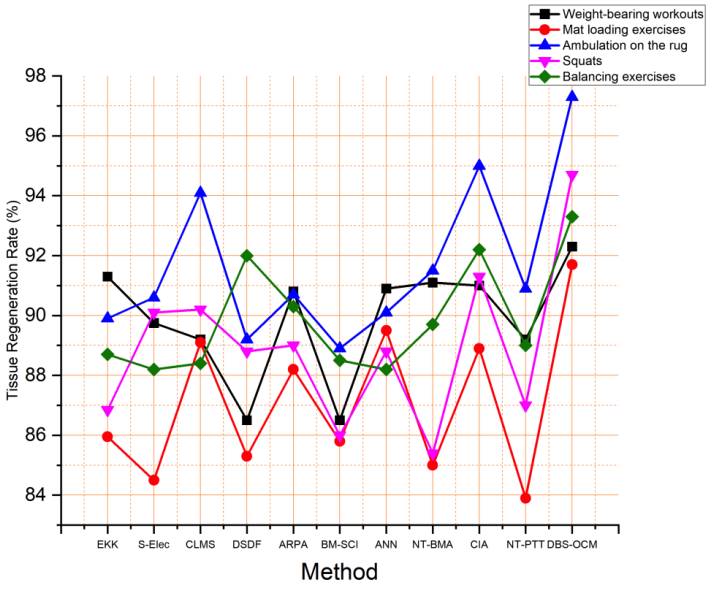

Figure 5. Tissue regeneration rate analysis.

$$TGR = \frac{M_f - M_i}{M_i} \times 100 \tag{18}$$

The final and first tissue measurements are denoted M_f *and* M_i. The DBS-OCM approach performs better than other procedures, with an average Tissue Regeneration Rate of 93.9%. The exceptional achievement is ascribed to the DBS-OCM, which enables improved tissue regeneration during VR Exercise Rehabilitation with OCM in contrast to traditional methods.

Figure 6 illustrates the percentage increase in the effectiveness of resistance training improvement for Weight-bearing workouts, mat-loading exercises, Ambulation on the rug, Squats, and Balancing exercises across various techniques. The effectiveness of resistance training improvement is computed using Equation (19).

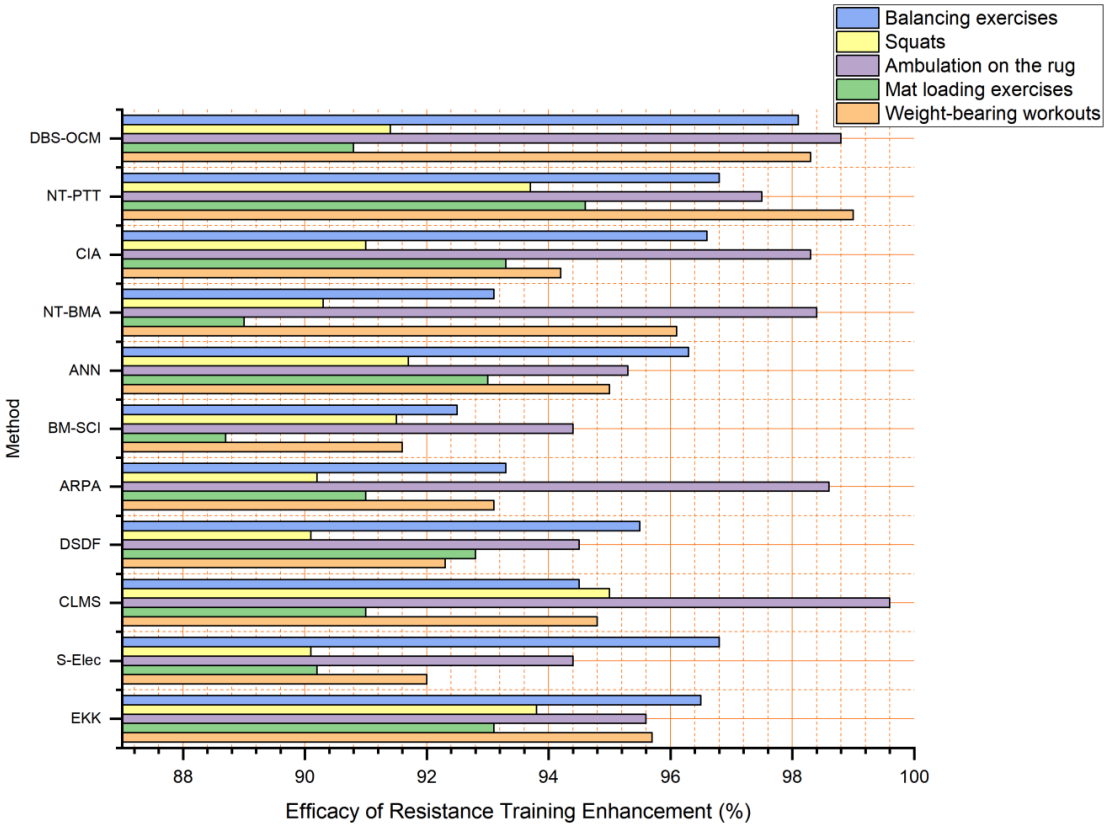

Figure 6. Efficacy of resistance training improvement analysis.

$$ERTE = \frac{T_{post} - T_{pre}}{T_{pre}} \times 100 \tag{19}$$

The post and pre-training strength are expressed T_{post} *and* T_{pre}. The DBS-OCM approach, on average, exhibits a higher level of performance, as shown by an Efficacy of Resistance Training Improvement of 95.5%. Significant progress is ascribed to the DBS-OCM, which enhances the effectiveness of resistance training in VR Exercise Rehabilitation with OCM compared to conventional approaches.

Figure 7 depicts the percentage increase in participant engagement for different techniques, including Weight-bearing workouts, mat-loading exercises, Ambulation

on the rug, Squats, and Balancing exercises. The participant engagement boost is calculated using Equation (20).

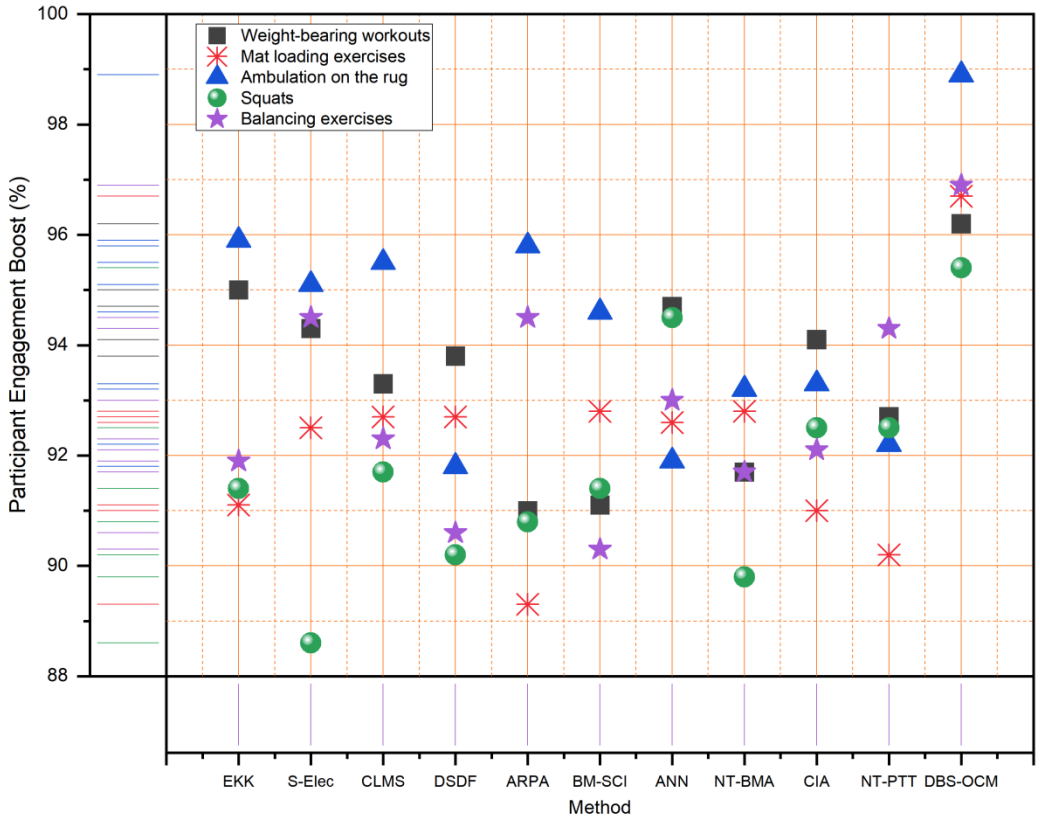

Figure 7. Participant engagement boost analysis.

$$PEB = \frac{E_{post} - E_{pre}}{E_{pre}} \times 100 \tag{20}$$

The pre- and post-participant engagement are expressed E_{pre} and E_{post}. On average, the DBS-OCM strategy demonstrates a higher level of Participant Involvement Boost, with a fantastic mean value of 96.8%. The significant improvement seen in participant involvement during VR Exercise Rehabilitation with OCM is credited to the DBS-OCM, demonstrating its effectiveness compared to traditional approaches.

Figure 8 illustrates the percentage of Flexibility Optimization achieved by the Biofeedback System across several approaches and Weight-bearing workouts, mat-loading exercises, Ambulation on the rug, Squats, and Balancing exercises. The Flexibility Optimization achieved by the Biofeedback System is computed using Equation (21).

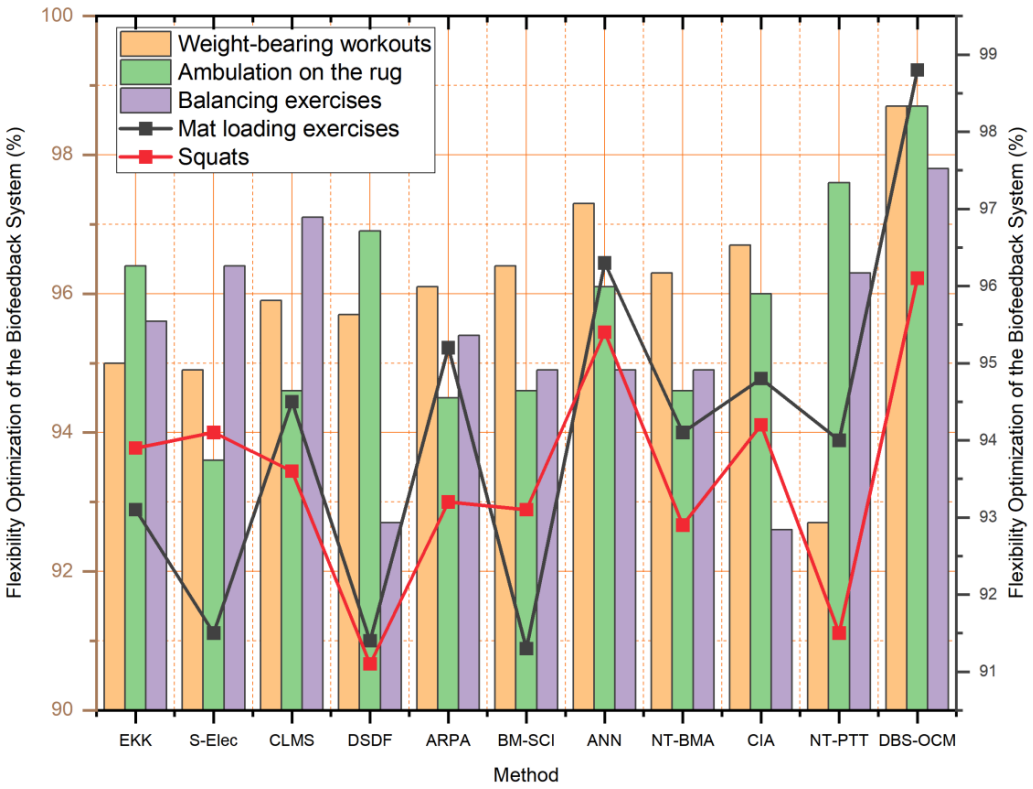

Figure 8. Flexibility optimization achieved by the biofeedback system analysis.

$$FO = \frac{F_{post} - F_{pre}}{F_{pre}} \times 100 \tag{21}$$

The pre and post-flexibility are expressed F_{pre} and F_{post}. The DBS-OCM technique regularly performs better than other methodologies, with an average Flexibility Optimization rate of 98.4%. The significant enhancement seen in this study demonstrates the effectiveness of using DBS-OCM to enhance the flexibility of the structure, exceeding conventional approaches in a diverse range of persons with OCM and VR Exercise Rehabilitation.

Figure 9 depicts the percentage impact on heart rates during virtual reality exercise rehabilitation for different approaches, as assessed on Weight-bearing workouts, mat-loading exercises, Ambulation on the rug, Squats, and Balancing exercises. The impact on heart rates during virtual reality exercise rehabilitation is calculated using Equation (22).

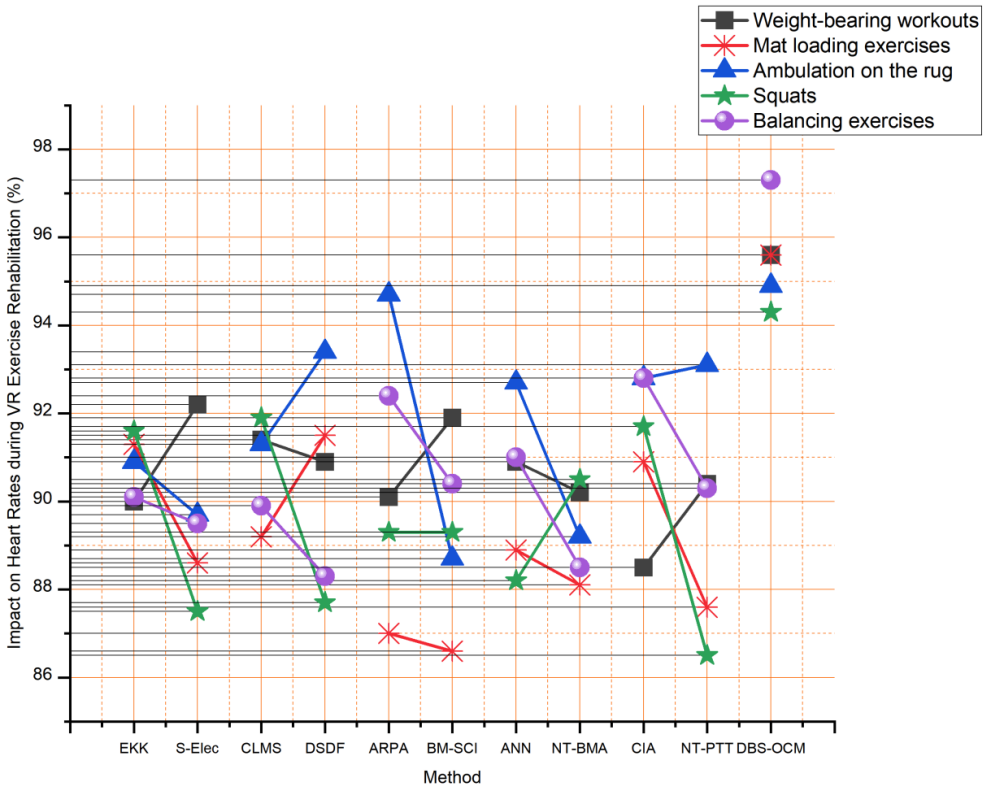

Figure 9. Impact on heart rates during VR exercise rehabilitation analysis.

$$IHR = \frac{HR_{post} - HR_{pre}}{HR_{pre}} \times 100 \tag{22}$$

The pre and post heart rate are expressed HR_{pre} *and* HR_{post}. The DBS-OCM approach routinely exhibits exceptional performance, as seen by an average Impact on Heart Rates of 95.5%. The significant improvement shown in this study highlights the efficacy of using DBS-OCM in modulating heart rates during VR Exercise Rehabilitation with OCM for persons of various backgrounds, surpassing the efficiency of conventional approaches.

Wound closure rate, cellular activity, and healing rate are metrics for tissue regeneration. These parameters are crucial for assessing rehabilitation progress and enabling DBS-OCM to offer adaptive and focused treatment to optimise recovery results in virtual reality environments. The DBS-OCM method demonstrates noteworthy performance across multiple metrics, including Tissue Regeneration Rate (93.9%), Efficacy of Resistance Training Enhancement (95.5%), Participant Engagement Boost (96.8%), Flexibility Optimization of the Biofeedback System (98.4%), and Impact on Heart Rates during VR Exercise Rehabilitation (95.5%). The results underscore the suggested approach's strong performance and advantages, placing it as a potential innovation in Virtual Reality Exercise Rehabilitation. OCMs are great for many training uses because of their high tensile strength, flexibility, and wear resistance. Due to these qualities, the effectiveness and durability of DBS-OCM devices are ensured throughout lengthy periods of rehabilitation.

5. Conclusion and future study

Exercise Rehabilitation's importance in preserving and improving physical fitness is paramount for holistic wellness. Incorporating OCM presents a new paradigm, capitalizing on their distinct characteristics in tissue regeneration. The significance of Biofeedback Systems in enhancing VR Exercise Rehabilitation is of utmost importance, as they provide a customized and efficient methodology. The Design of Biofeedback System-driven Optoelectronic Conjugate Materials (DBS-OCM) is a planned study that aims to synthesize and analyze OCM, explicitly focusing on their potential function in tissue healing. The system's adaptability is enhanced by the design and preparation technique of the resistance trainer, as well as the investigation of strain rate in polyacetylene materials. Integrating VR sessions enhances the level of immersion experienced. The experimental findings show significant progress, such as a tissue regeneration rate of 93.9%, an improvement of 95.5% in the effectiveness of resistance training, a 96.8% increase in participant involvement, and a 98.4% enhancement in optimizing flexibility within the Biofeedback System. VR Exercise Rehabilitation has been shown to significantly impact heart rates, resulting in a noteworthy improvement of 95.5%.

The results demonstrate the effectiveness of DBS-OCM in transforming VR Exercise Rehabilitation. Acknowledging and tackling several obstacles and concerns, including managing individual variability and effectively enhancing the system's flexibility, is essential. The manifold advantages and auspicious results present DBS-OCM as an innovative methodology with substantial potential for influencing the trajectory of Exercise Rehabilitation.

Ethical approval: Not applicable.

Conflict of interest: The author declares no conflict of interest.

References

1. Führer, T., Kliegl, R., Arntz, F., Kriemler, S., & Granacher, U. (2021). An update on secular trends in physical fitness of children and adolescents from 1972 to 2015: a systematic review. Sports Medicine, 51, 303-320.
2. Bo, W., Xi, Y., & Tian, Z. (2021). The role of exercise in rehabilitation of discharged COVID-19 patients. Sports Medicine and Health Science, 3(4), 194-201.
3. Wan, Y., Ramirez, F., Zhang, X., Nguyen, T. Q., Bazan, G. C., & Lu, G. (2021). Data-driven discovery of conjugated polyelectrolytes for optoelectronic and photocatalytic applications. npj Computational Materials, 7(1), 69.
4. Opoku, H., Choy, J. Y., Kumar, K. A., Shrestha, N. K., Rabani, I., Patil, S. A., ... & Bathula, C. (2021). Facile synthesis and optoelectronic properties of thienopyrroledione based conjugated polymer for organic field-effect transistors. Dyes and Pigments, 186, 108973.
5. Tang, N., Zheng, Y., Cui, D., & Haick, H. (2021). Multifunctional dressing for wound diagnosis and rehabilitation. Advanced Healthcare Materials, 10(22), 2101292.
6. Belcher, B. R., Zink, J., Azad, A., Campbell, C. E., Chakravartti, S. P., & Herting, M. M. (2021). The roles of physical activity, exercise, and fitness in promoting resilience during adolescence: effects on mental well-being and brain development. Biological psychiatry: Cognitive neuroscience and neuroimaging, 6(2), 225-237.
7. Jimeno-Almazán, A., Franco-López, F., Buendía-Romero, Á., Martínez-Cava, A., Sánchez-Agar, J. A., Sánchez-Alcaraz Martínez, B. J., ... & Pallarés, J. G. (2022). Rehabilitation for post-COVID-19 condition through a supervised exercise intervention: A randomized controlled trial. Scandinavian journal of medicine & science in sports, 32(12), 1791-1801.

8. Alnajjar, F., Zaier, R., Khalid, S., & Gochoo, M. (2021). Trends and technologies in the rehabilitation of foot drop: A systematic review. Expert review of medical devices, 18(1), 31-46.
9. Feng, R., Niu, P., Hou, B., Wang, Q., Jia, L., Lin, M., & Li, D. (2022). Synthesis and characterization of the flower-like LaxCe1− xO1. 5+ δ catalyst for low-temperature oxidative coupling of methane. Journal of Energy Chemistry, 67, 342-353.
10. Srinithi, S., Arumugam, B., Chen, S. M., Annamalai, S., & Ramaraj, S. K. (2023). Synthesis and characterization of pyrochlore-type lanthanum cerate nanoparticles: Electrochemical determination of antibiotic drug sulfadiazine in biological and environmental samples. Materials Chemistry and Physics, 296, 127244.
11. El Fezazi, M., Achmamad, A., Jbari, A., & Jilbab, A. (2023). A convenient approach for knee kinematics assessment using wearable inertial sensors during home-based rehabilitation: Validation with an optoelectronic system. Scientific African, 20, e01676.
12. Kim, J. J., Wang, Y., Wang, H., Lee, S., Yokota, T., & Someya, T. (2021). Skin electronics: next-generation device platform for virtual and augmented reality. Advanced Functional Materials, 31(39), 2009602.
13. Zhang, G., Chen, Y., Zhou, W., Chen, C., & Liu, Y. (2023). Bioenergy-Based Closed-Loop Medical Systems for the Integration of Treatment, Monitoring, and Feedback. Small Science, 3(10), 2300043.
14. Madrigal, J. A. B., Rodríguez, L. A. C., Pérez, E. C., Rodríguez, P. R. H., & Sossa, H. (2023). Hip and lower limbs 3D motion tracking using a double-stage data fusion algorithm for IMU/MARG-based wearables sensors. Biomedical Signal Processing and Control, 86, 104938.
15. Huang, Y. C., Hsu, C. C., Fu, T. C., & Wang, J. S. (2023). Interval aerobic/resistance exercise training depresses adrenergic-induced apoptosis of lymphocytes in sedentary males. European Journal of Applied Physiology, 1-12.
16. Kiyotake, E. A., Martin, M. D., & Detamore, M. S. (2022). Regenerative rehabilitation with conductive biomaterials for spinal cord injury. Acta biomaterialia, 139, 43-64.
17. Al-Waeli, K. H., Ramli, R., Haris, S. M., Zulkoffli, Z. B., & Amiri, M. S. (2021). Offline ANN-PID controller tuning on a multi-joint lower limb exoskeleton for gait rehabilitation. IEEE Access, 9, 107360-107374.
18. He, J., Jin, S., Fan, W., Wu, L., Gopinath, S. C., & Hu, Z. (2022). Nanotechnology-assisted biomarker analysis to rehabilitate acute ischemic stroke patients by early detection. Process Biochemistry, 114, 28-35.
19. Zhao, Y., Gu, W., Zhang, H., Sun, J., Ma, W., Dong, Y., & Nie, J. (2022). Enriched rehabilitation training can improve the cognitive dysfunction of chronic cerebral hypoperfusion rats. Neuroscience Informatics, 2(2), 100050.
20. Wang, B., & Deng, X. (2021). Nanotube research combined exercise rehabilitation therapy to treat knee arthritis in football players. International Journal of Nanotechnology, 18(1-4), 29-39. https://partners.natus.com/